Muonium defect levels in Czochralski-grown silicon-germanium alloys

B. R. Carroll,[1,*,†] R. L. Lichti,[1] P. J. C. King,[2] Y. G. Celebi,[1,3] I. Yonenaga,[4] and K. H. Chow[5]
[1]*Department of Physics, Texas Tech University, Lubbock, Texas 79409-1051, USA*
[2]*STFC ISIS Facility, Rutherford Appleton Laboratory, Chilton, Oxfordshire OX11 0QX, United Kingdom*
[3]*Department of Physics, Istanbul University, Vezneciler, 34134 Istanbul, Turkey*
[4]*Institute for Materials Research, Tohoku University, Sendai, Miyagi 980-8577 Japan*
[5]*Department of Physics, University of Alberta, Edmonton, Canada T6G 2G7*
(Received 7 April 2010; revised manuscript received 8 July 2010; published 10 November 2010)

We report Muonium (Mu) donor and acceptor levels in Czochralski-grown Silicon Germanium alloys (Cz-$Si_{1-x}Ge_x$). Measurement of these defect energies provides an analogous examination of Hydrogen defects that are otherwise inaccessible. Temperature-dependent Muonium fractions in several alloy samples (x =0.20,0.45,0.77,0.81,0.84,0.90,0.91,0.94,0.98) show charge-state transitions assigned to Mu donor and acceptor ionizations. Our results indicate a deep Mu donor level across the alloy system. The Mu acceptor level is deep in pure Si and valence-band resonant in pure Ge; we specifically examine the compositional dependence of the Mu_T^0 acceptor ionization energy in Ge-rich alloys, where this level crosses into the valence band.

DOI: 10.1103/PhysRevB.82.205205 PACS number(s): 36.10.Ee, 71.55.Ak, 61.72.uf

I. INTRODUCTION

Passivation behavior of hydrogen in semiconductors has become an important issue in device manufacture. Hydrogen is an unavoidable impurity introduced during many materials processing techniques but is also intentionally introduced to remove unwanted interface-related defect levels. The dopant behavior of interstitial H can considerably affect the electrical and optical characteristics of a semiconductor host, however, examination of many monatomic H defect properties has proven elusive. The high reactivity and mobility of H hinders observations of the isolated defect. Observation of H defect levels in silicon-germanium alloys may reveal the origin of difficulties associated with H treatments in these technologically important materials.[1] We have therefore examined defect behaviors of the Mu analog of H in Czochralski-grown $Si_{1-x}Ge_x$ to pursue the possibility that the introduction of H may produce electrically active defects instead of passivating existing defects.

The dopant behavior of H in SiGe alloys is of particular importance in the realization of high-mobility transistors and efficient photovoltaics. Passivation of deleterious electrical impurities in Ge-rich materials has been pathological to say the least. Estreicher and Maric[2] suggest, based on the relative stability of H_{BC}^0 and H_T^0, that the inability of H to properly passivate defects after hydrogenation compared to Si is due to the lack of H^+ and high formation probability of H_2. First-principles calculations of Van de Walle and Neugebauer[3] predict that H^- is the thermodynamically stable form of monatomic H in Ge unlike the amphoteric behavior of H in Si. Furthermore, Weber *et al.*[1] have calculated that Ge dangling bonds ought to have a level deep in the valence band (VB) resulting in exclusively negatively charged configurations. In addition, an isolated Si impurity in Ge is known to be a trap for H^-, which activates Si to become a shallow acceptor[4,5] thus the Si-H pair may be in the negative charge state in Ge-rich alloys for ordinary device operating conditions. Of the numerous explanations for the ineffectiveness of H passivation in Ge, we seek to experimentally investigate the defect behavior of H across the full $Si_{1-x}Ge_x$ composition range with Muonium techniques.

Muonium is the chemical species consisting of a positively charged muon nucleus with a bound electron. This novel atom is observed by means of muon spin research (μSR), which involves implanting spin-polarized positive muons and detecting the positrons emitted when the muons decay (see Chow *et al.*[6] for brief review). The positrons from the muon decay process are preferentially emitted along the muon spin direction so that their detection provides a means of measuring the muon polarization evolution in a sample. In particular, this process allows muon and muonium defect states (analogs of the H defect states) to be characterized in semiconducting materials. The majority of μSR results in group-IV semiconductors can be explained by three Mu charge states and two interstitial locations (the bond-centered, BC, site and the large tetrahedral, T, void): the atomic species Mu_{BC}^0 and Mu_T^0, as well as the ions Mu_{BC}^+ and Mu_T^-. The similar electronic and spin characteristics of H and Mu as well as the near equivalence of purely electronic energies makes the Mu analogy valid concerning ionization processes and spin dynamics. The Mu analogy with H is less valid with respect to the motional dynamics of these atoms since the muon is 1/9th the mass of a proton, thereby resulting in a higher zero-point energy and diffusivity of muonium compared to protium (^{1}H) and more so for the heavier H isotopes.

This work intends to identify Mu ionization processes in samples that span the full alloy range. Prior results place the Mu_{BC} donor level in Si at 210 ± 10 meV below the conduction-band minimum[7] and the Mu_T acceptor level 600 ± 40 meV below the conduction-band minimum.[8] These results are consistent with the analogous H energies determined by deep level transient spectroscopy (DLTS) measurements following proton incorporation.[9,10] In pure germanium, however, only the H donor level has been observed with DLTS.[11] The H acceptor level is predicted to be shallow or valence band resonant and thus inaccessible to DLTS. The Mu acceptor level was assigned by Lichti *et al.*[12,13] to be

80 ± 10 meV below the valence-band maximum in Ge. The donor level in Ge has recently been placed[13] at 145 ± 7 meV below the conduction-band minimum based on separation of Mu_T^- and Mu_{BC}^+ components under optical excitation. We note that this value is consistent with the 175 meV ionization energy[12] associated with $Mu_T^0 \rightarrow Mu_{BC}^+$ if one assumes the roughly 30 meV $T \rightarrow BC$ transition barrier for a Mu^0 site change plus Mu_{BC} ionization.

Both H and Mu exhibit negative-U characteristics in $Si_{1-x}Ge_x$. Experimentally, U is defined by the difference between the acceptor $[0/-]$ and donor $[+/0]$ defect level energies, $U=A[0/-]-D[+/0]$. In this regime neutral species are always metastable, thus the thermodynamically stable charge state of H switches directly from H^+ to H^- at the $H[+/-]$ level with increasing Fermi energy. The nonequilibrium nature of our μSR experiments allows for observation of metastable Mu species but no direct measure of thermodynamically stable states. The BC donor and T-site acceptor levels may be measured by μSR techniques from the ionization of neutral species. Placement of donor and acceptor levels with respect to a host's bandgap determines the $[+/-]$ energy level, from which one can predict the dopant behavior of H(Mu). With all three thermodynamic energy levels within the band gap of a material (e.g., pure Si), H(Mu) acts as a deep, compensating center. One issue in Ge, however, has been the determination of $H[0/-]$ and $H[+/-]$ levels. If both are resonant with the valence band, H would explicitly form H^- in equilibrium thus exclusively functioning as a shallow acceptor with the H^- core capturing a weakly bound VB-like hole at low temperatures. With only $H[0/-]$ resonant with the valence band, H retains its compensating behavior.

For the muonium analog, Mu_T^0 is typically formed by epithermal electron capture from the implantation ionization track and may then form a metastable shallow acceptor configuration if the T-site acceptor level is valence-band resonant, independent of the Fermi level position. One would naively expect a rather rapid $Mu_T^0 \rightarrow Mu_T^-$ transition in Ge if the analogous $Mu[0/-]$ level is valence-band resonant. However, the Mu_T^0 lifetimes can be extremely long due to the very different motional properties of the two charge states. The T-site neutral is extremely mobile at all temperatures and this rapid motion must be disrupted by some mechanism (e.g., scattering) in order to capture a second electron to form the very immobile Mu_T^-

Although bond-centered H has been observed by techniques such as Fourier transform infrared spectroscopy (FTIR),[14,15] the high diffusivity of T-site H compared to necessary experimental time scales makes the measurement of $H[0/-]$ inaccessible to conventional techniques. This provides a unique opportunity for muonium experiments to elucidate the issue of hydrogen's inability to passivate deleterious charged defects in Ge-rich alloys. We have explicitly sought to observe the disappearance of the bond-centered and tetrahedral muonium signals corresponding to electron and hole ionization, respectively. These measurements have been performed using transverse field spectroscopy (TF-μSR) and muonium resonance (RF-μSR) techniques. We have observed the crossing of the $Mu[0/-]$ level into the valence band[16] with increasing Ge content that indicates Mu may form a shallow acceptor in the T-site location at low temperatures for $x>0.92$. We find that the $Mu[+/-]$ level is well into the band gap for all alloy compositions indicating that Mu or H should act as a deep, compensating center across the full alloy range. King *et al.*[17,18] have reported results concerning the compositional dependence of Mu hyperfine (HF) parameters as well as the determination of acceptor levels in a few Ge-rich samples. In continuing this investigation, we have examined Mu ionization processes in a larger collection of samples.

II. EXPERIMENTAL DETAILS

The μSR method consists of 100% spin-polarized positive muons (μ^+) implanted in a given sample under a variety of possible field configurations; the time-dependent muon decay is observed by scintillating positron detectors arranged around the sample. The angular distribution of decay positrons averaged over all possible kinetic energies results in an anisotropy along the muon spin direction. Since the positrons are emitted preferentially along the muon spin at a given decay time, the time-dependent asymmetry of positron counts for experiments consisting of several million muon decay events is an effective means of measuring muon spin rotation, relaxation, and resonance phenomena.

A. Sample information

Our study has focused on Czochralski-grown silicon-germanium alloys grown by Yonenaga at the Tohoku University Institute of Materials Research. These are nominally undoped samples with net carrier concentrations of roughly $10^{14}-10^{15}$ cm^{-3}; our Si-rich samples ($x=0.11$ and 0.20) have n-type conductivity and Ge-rich samples ($x=0.55$, 0.77, 0.81, 0.84, 0.90, 0.91, and 0.98) have p-type conductivity. The source of p-type conductivity has not been established. Being Cz samples grown in a quartz crucible, oxygen impurities likely play a role in the Mu dynamics. Without examining the dependence of μSR signals as a function of impurity content for a given alloy composition, the extent to which Mu state fractions and transitions are affected by the common Cz-introduced impurities cannot be determined.

A critical concern in examining Czochralski-grown samples is the role of interstitial oxygen incorporated from the quartz crucible. Oxygen in $Si_{1-x}Ge_x$ primarily forms a IV-O-IV "quasimolecule." In Si, it has been found from IR spectroscopy and first-principles calculations that the oxygen complex (Si-O-Si) is nearly linear with O nominally at the bond-centered location.[19] Oxygen in Ge is delocalized about a torus normal to the Ge-Ge bond and centered at the BC location.[20] These defect complexes, although differing in bond angle (i.e., symmetry), show IR absorption lines associated with the Si-O-Si and Ge-O-Ge stretch modes at 1106 cm^{-1} and 855 cm^{-1}, respectively. Yonenaga *et al.*[21] observed by FTIR and secondary-ion-mass spectroscopy (SIMS) that in their Si-rich alloys, nearly all oxygen is found in a Si-O-Si configuration. Only the stretch mode from Si-O-Si is present with an absorption coefficient consistent with the total oxygen concentration determined by SIMS. In Ge-rich alloys, the Si-O-Si mode at 1106 cm^{-1} is seen but the

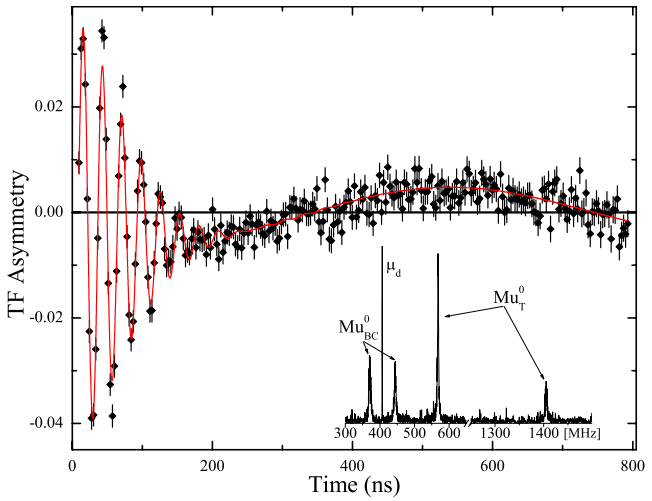

FIG. 1. (Color online) Raw HTF-μSR time spectrum in a rotating reference frame (RRF) observed in $x=0.20$ at 55 K with an applied field of 3 T. Fast relaxing component at early times is due to the ν_{12} and ν_{34} signals of Mu^0_{BC}. The weak, persisting signal is the Larmor precession of diamagnetic muonium states. RRF frequency (405 MHz) was set slightly below that of the diamagnetic precession to accentuate the BC and diamagnetic components. (Inset) Fast Fourier transform of the full time spectrum for this data run. Diamagnetic line is truncated to clearly illustrate the paramagnetic signals.

local vibrational modes associated with the puckered Ge-O-Ge or Ge-O-Si complexes are not observed, providing rather convincing evidence that oxygen strongly prefers Si-Si bonds.

B. Transverse field experiments

We have investigated paramagnetic muonium signals in the high field limit (i.e., Paschen-Back regime) where energy splittings of the ν_{12} and ν_{34} transition are sufficiently decoupled from spin-orbit interactions. The resulting precession frequencies of paramagnetic muonium species are given by[22]

$$\nu_{\mathrm{Mu}} \approx \left| \nu_\mu \mp \frac{A}{2} + \frac{A^2}{4\nu_e} \right|, \tag{1}$$

where ν_μ is the muon Larmor frequency of diamagnetic Mu (labeled μ_d in Fig. 1). High transverse field (HTF-μSR) experiments were performed on the M15 beamline at the TRIUMF facility (Vancouver, Canada) with the HiTime spectrometer. Our measurements were performed on several Cz-$Si_{1-x}Ge_x$ samples cut specifically for the HiTime spectrometer ($x=0.20$, 0.45, 0.77, 0.84, 0.90, and 0.98); samples are nominally disk shaped with diameters of $\sim 5-7$ mm and ~ 1 mm thicknesses. An external field of 3 T was applied perpendicular to the initial muon spin direction with the temperature controlled by a horizontal flow cryostat.

The high timing resolution provided by these HTF-μSR experiments allows for the spectroscopic identification of paramagnetic muonium configurations. Due to phase coherency restrictions inherent in TF-μSR, these measurements are only sensitive to muonium states formed promptly upon implantation. Figure 1 shows an example time spectrum and fast Fourier transform of muonium determined by the HTF-μSR technique.

The tetrahedral Mu atom in $Si_{1-x}Ge_x$ has a nominally isotropic HF interaction; the bond-centered Mu has a hyperfine interaction with anisotropy along one of the four $\langle 111 \rangle$ bond directions that gives rise to orientation-dependent μSR signals with HF frequencies determined by

$$A_{\mathrm{BC}}(\theta_i) = A_{iso} + \sum_{i=1}^{4} \frac{D}{2}(3\cos^2\theta_i - 1), \tag{2}$$

where θ_i is the angle between the applied magnetic field and bond direction of the ith BC configuration. Samples are nominally aligned with the applied field along the [100] crystaligraphic axis. In this configuration $3\cos^2\theta - 1 = 0$ for all four BC orientations, thus all BC signals have a HF interaction of A_{iso}. Although this provides no information on the dipolar component of the HF interaction, identification of the BC species is simplified and we may unambiguously observe the temperature-dependence of Mu^0_{BC}.

C. Muonium resonance experiments

Muonium spin resonance measurements were performed using the traditional nuclear magnetic resonance configuration. Muons are implanted with the initial polarization along a longitudinal applied magnetic field with an RF excitation in the plane transverse to muon spin polarization. The RF coils provide a means to drive a resonant muon spin-flip transition where the RF-μSR signal is determined by the difference in time-evolved muon spin polarization with the RF on and off. Since the longitudinal applied field configuration used in these RF-μSR experiments does not require initial phase coherency, this technique is sensitive to both prompt and slowly formed Mu states. Comparison of the promptly formed Mu signals observed by TF-μSR to those of RF-μSR can reveal the presence of Mu species formed after the initial thermalization.

Our reported RF-μSR experiments were performed on the M20 beamline at TRIUMF and the EMU beamline at ISIS. Investigations of paramagnetic signals at ISIS were taken with a constant RF frequency of 500 MHz and magnetic field sweeps were performed in the region of the ν_{12} resonance. These Mu resonance experiments were focused on observing HF distributions of Mu_{BC} and Mu_T in Ge-rich alloys to identify paramagnetic configurations and furthermore measuring the temperature-dependent diamagnetic Mu fraction resulting from charge-state transitions. Individual RF-μSR resonances are described by the following Lorentzian peak function:

$$A_{\mathrm{RF}} = A\frac{\omega_1^2}{\zeta_\mu^2 + \Delta\omega^2 + \omega_1^2}, \tag{3}$$

where A is the peak resonance amplitude, ζ_μ is the inverse muon lifetime plus any chemical transition rate, ω_1 is the RF frequency, and $\Delta\omega$ is the difference between the driving frequency and muon Larmor or HF precession frequency due to the applied longitudinal field. Figure 2 shows example resonance curves obtained with the field-swept RF-μSR tech-

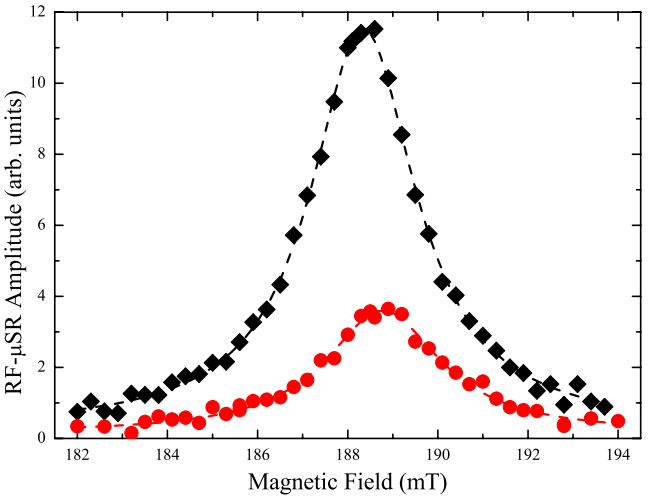

FIG. 2. (Color online) Magnetic field swept RF-μSR resonances of diamagnetic Mu in $Si_{0.09}Ge_{0.91}$ at 290 K (diamonds) and 25 K (circles). These data were obtained with an RF frequency of 25.5 MHz. Dashed lines are fits to Lorentzian peak function.

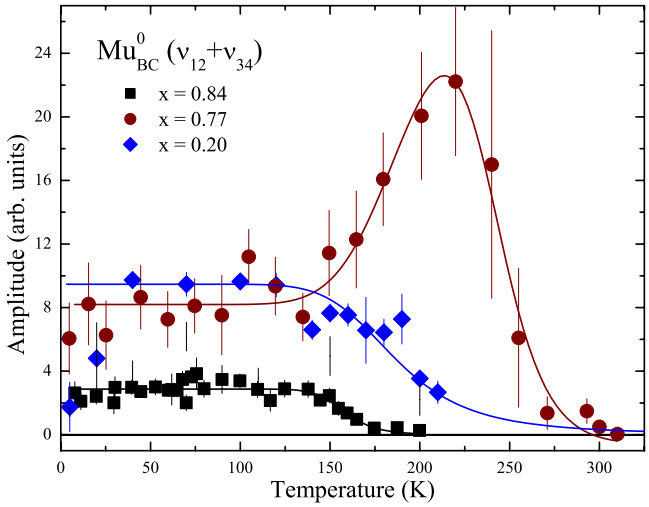

FIG. 3. (Color online) Temperature-dependent Mu_{BC} amplitudes for $x=0.20$, 0.77, and 0.84 determined by HTF-μSR measurements. Solid lines for $x=0.84$ & 0.20 are fits to Eq. (4); solid line for $x=0.77$ is from a fit to Eq. (4) with an additional thermally activated term to account for the site-change transition.

nique. Our resonance experiments were concerned with measuring the temperature dependence of the peak amplitude for diamagnetic and paramagnetic Mu resonances. In particular, temperature-dependent Mu^0 fractions for both interstitial sites as well as the ionic charge states are needed to understand the chemical pathway for muonium disappearance, i.e., charge-state transitions, site changes, or a combination of these.

III. RESULTS AND ANALYSIS

The HF spectra and RF-resonance curves of our samples have shown features consistent with pure charge-state transitions. Several Ge-rich samples show weak paramagnetic signals in HTF-μSR measurements due to fast spin relaxation such that an accurate ionization energy could not be determined. Assignment of donor and acceptor levels may still eventually be possible by examination of cyclic processes in Longitudinal Field μSR (LF-μSR) and low-field TF-μSR. Spectroscopic identification of diamagnetic charge states is not possible. However, separation of the two components (Mu^-_T and Mu^+_{BC}) was accomplished in Ge by photoexcited TF-μSR techniques.[23] Attempts to use Optical TF-μSR techniques on these alloys were unsuccessful, presumably because recombination is too rapid.

In cases where only the charge-state transition is observed, the muonium ionization energies are obtained in both TF- and RF-μSR measurements from temperature-dependent Mu fractions with the following time-integrated expression

$$A(T) = A_0 - A_i \frac{\nu_i}{\nu_i + \nu_\mu}, \tag{4}$$

where $\nu_i = \nu_i^0 \exp(\frac{-E_i}{kT})$ is the ionization rate and ν_μ is the inverse muon lifetime.[8,24] For situations where multiple transition processes are observed (e.g., Mu^0_{BC} in $x=0.77$), additional terms of this form are added to account for each transition in the temperature-dependent amplitude; that is, Eq. (4) becomes a sum over the index i. We have yet to determine Mu[0/−] in our mid-range alloys ($0.2<x<0.77$) because site-change energies between the two neutral species ($T \rightarrow BC$) are lower than the charge-state transition energies, thus no charge-state transition is directly observed in TF- and RF-μSR. Further experimentation will be needed to determine Mu acceptor levels in this alloy region.

A. Mu ionization energies from HTF-μSR

Three samples ($x=0.20$, 0.77, and 0.84) show clear spectroscopic indications of BC muonium signals in HTF-μSR. The extrapolated zero-temperature HF frequencies are: $A_{iso}=73.2$ MHz, 90.2 MHz, and 92.2 MHz, respectively.[25] Figure 3 displays the observed Mu^0_{BC} fraction as a function of temperature for these three samples. No increase in T-site muonium is evident, thus the disappearance of these paramagnetic signals is assigned to donor ionization. Indeed, we assign the disappearance of Mu^0_{BC} to electron ionization over the full alloy composition range. Donor levels have been determined from both the disappearance of Mu_{BC} and growth of the Mu^+_{BC} diamagnetic signal. The temperature-dependent amplitude of Mu^0_{BC} in $x=0.20$ and 0.84 show a straightforward disappearance with ionization energies of 206 ± 4 meV and 340 ± 74 meV, respectively; fitted frequency prefactors (ν_i^0 from Eq. (4)) are 3.5×10^{13} Hz and 3.3×10^9 Hz, respectively. The low-temperature behavior of Mu^0_{BC} in $x=0.20$ shows an amplitude increase from 5 to 40 K of unknown origins. Similar features are observed in several other $Si_{1-x}Ge_x$ samples; since the charge-state transitions assigned to donor and acceptor ionization energies are often far removed in temperature from these low-temperature features, these regions are at present excluded from our fits.

Our measurements in the $x=0.20$ sample did not go to sufficiently high temperatures to see the full Mu^0_T disappear-

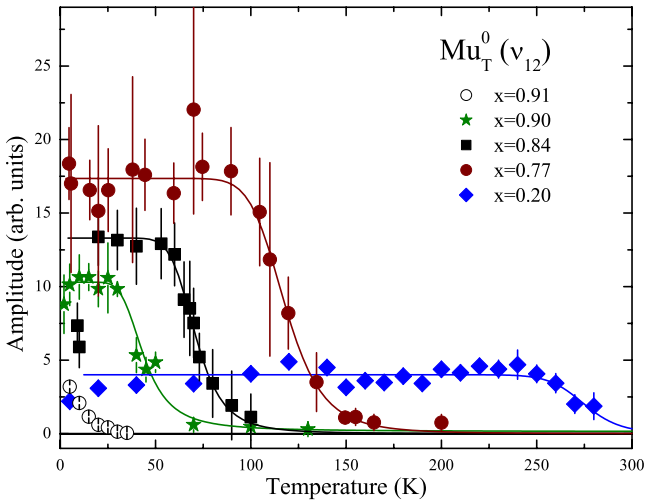

FIG. 4. (Color online) Temperature-dependent Mu_T^0 amplitude determined by HTF-μSR (x=0.20, 0.77, 0.84, and 0.90) and RF-μSR (x=0.91). Solid lines are fits to Eq. (4); note, the lowest temperature points for x=0.84 were omitted in fitting.

ance. Based on the known T-to-BC site change energy in pure Si, this feature in x=0.20 is most likely due to site change rather than acceptor ionization. For alloy samples with Ge fractions above 77%, the T-to-BC site change energy is higher than that of the Mu_T acceptor ionization energy.[16] This allows for the direct measure of the acceptor energy with respect to the valence band maximum. The Mu site-change in x=0.77 is illustrated (Fig. 3) by the rise in Mu_{BC}^0 fraction near 150K that comes from the disappearance of Mu_T^0. Above this alloy concentration, the Mu_T^0 disappearance has no corresponding rise in Mu_{BC}^0 fraction. In this region ($0.77<x<1$) we assign the temperature-dependent disappearance of the T-site neutral species to a hole ionization process thus defining the Mu acceptor level. King *et al.*[16] previously reported Mu acceptor levels in x=0.77, 0.84, and 0.90 samples. These are 128 ± 8 meV, 73 ± 10 meV, and 22 ± 2 meV, respectively; fitted frequency prefactors are 7.4×10^{10} Hz, 9.0×10^{9} Hz, and 2.3×10^{8} Hz, respectively. We have continued this work by using the same μSR techniques to observe the disappearance of Mu_T in x=0.81. From this temperature-dependent Mu_T amplitude, we obtain an acceptor energy of 116 ± 8 meV.

B. Mu defect levels from RF-μSR

Mu resonance experiments have been further pursued to compliment our HTF-μSR data and to identify ionization signatures that may be inaccessible to transverse field techniques. Using the RF-μSR method, we have observed the ν_{12} muon spin-flip resonance from Mu_T^0 as a function of temperature in $Si_{0.09}Ge_{0.91}$. Unlike the Mu_T^0 HF distribution of x=0.84 and 0.90 samples that show two resonant peaks,[16] the x=0.91 sample shows a single, broad resonance under an RF excitation of 500 MHz. The temperature dependence of the peak RF amplitude for this sample is included in Fig. 4. The fitted ionization energy from Eq. (4) is assigned to the Mu[0/−] acceptor level 4.5 ± 1 meV above the top of the valence band assuming that the 5 K amplitude is essentially the zero-temperature Mu_T fraction.

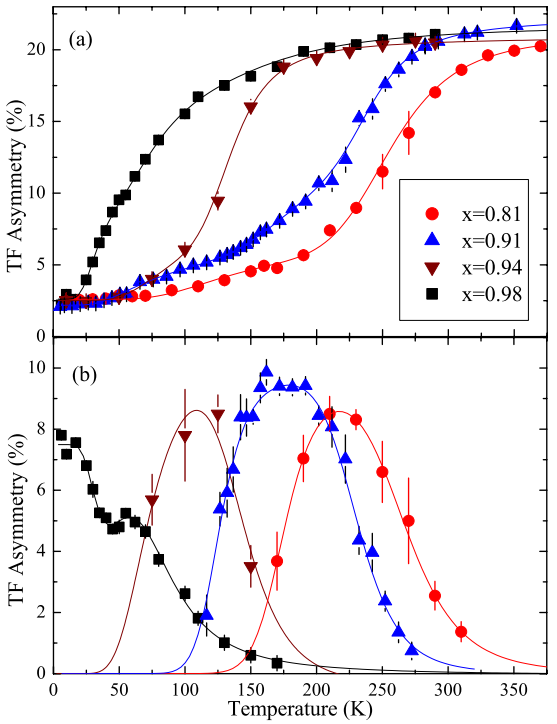

FIG. 5. (Color online) Temperature-dependent amplitudes of the (a) slow and (b) fast relaxing diamagnetic signals in several Ge-rich alloys with fitting results (solid lines). Note that the curve associated with x=0.94 in (b) is a guide to the eyes as there is insufficient data for any meaningful fit.

C. Low transverse-field results

Transverse-field experiments under a 10 mT applied field show precession signatures of the diamagnetic muonium configurations Mu^+ and Mu^-. Both diamagnetic configurations precess at the same frequency in TF-μSR, thus there is no direct indication of charge state in our spectra. Multiple diamagnetic signals can be decomposed from the raw data when relaxation rates or dynamic processes are significantly different. Two diamagnetic components are observed in Ge-rich alloys by their differing relaxation rates: a slowly relaxing fraction assigned to Mu_{BC}^+ and a fast relaxing fraction that is likely the product of a cyclic process involving a Mu_T^- final state and site changes between T and BC. The negative charge state of Mu in Silicon Germanium is only stable in the T-site location. During thermalization, most of the initial muonium forms the quickly diffusing Mu_T^0 in Ge-rich Silicon Germanium. In contrast, the negative charge state is highly immobile to well above room temperature, thus the transition between Mu_T^0 and Mu_T^- requires a scattering interaction or a site-change cycle as Mu^0 in order to lose enough kinetic energy to form the more stable Mu^- ion.

Figure 5 displays the temperature dependence of the observed diamagnetic signals. Figure 5(a) shows several temperature-dependent Mu_{BC}^+ fractions with a predominant growth at high temperatures due to donor ionization and

multiple features at low temperatures of unknown origin. In several of these samples, the weak, low temperature features partially obscure the initial diamagnetic growth due to the Mu^0_{BC}-to-Mu^+_{BC} ionization process. This adds extra uncertainty to these fits, however, donor energies obtained from these low TF-μSR measurements are correlated with the Mu^0_{BC} disappearance from HTF-μSR. Comparison of these data with the elemental host (Si and Ge) further corroborates our assignment of the predominant growth of the slowly relaxing diamagnetic fraction to $Mu^0_{BC} \rightarrow Mu^+_{BC} + e^-$ (i.e., donor ionization) as the higher temperature transition.

We assign the more rapidly relaxing diamagnetic signal [Fig. 5(b)] to Mu^-_T that results from the following process:

$$Mu^0_T \rightarrow Mu^0_{BC} \rightarrow Mu^-_T. \quad (5)$$

From our prior argument that kinetic energy from the precursor muonium must be lost by scattering or site changes, this diamagnetic signal might form from impurity scattering although the onset energies vary smoothly with composition suggesting a site change. The onset and disappearance of this feature are clearly dependent on alloy concentration with the energy barrier into the diamagnetic state decreasing with increasing Ge content and the transition energy associated with the loss of this rapidly relaxing signal trending with the Mu^+_{BC} ionization. The energy for this disappearance matches the increase in the slower relaxing fraction in Fig. 5(a). This feature supports the argument that a cycle through the BC site as a neutral is the relevant Mu^-_T formation process for this component; thus when BC ionization is rapid enough, Mu follows this favorable pathway and results in a final state of Mu^+_{BC} rather than Mu^-_T. Relaxation rates for the Mu^-_T signal decrease with increasing temperature, indicating that the disappearance of this signal is not simply a hole ionization process (i.e., $Mu^0_T \rightarrow Mu^-_T + h^+$). One likely possibility for this relaxation mechanism is the onset of a cyclic charge-state process where Mu^-_T repeatedly captures and releases a hole from the valence-band maximum.

IV. DISCUSSION

Our measured donor and acceptor levels are compiled in Table I. The deep donor level in the band gap indicates that the donor electron is localized in the near vicinity of the muon; most of the electron wave function is concentrated on the two bonded nearest neighbors. The HF frequencies of these BC signals are a small fraction of the free atom value due to this bonding configuration. The acceptor levels below $x \approx 0.90$ are similarly deep in the band gap with a substantially higher HF frequency (2010 MHz) indicating a fairly localized electron bound to the T-site muon nucleus. For samples with the acceptor level resonant with the valence band, muonium trapped at the T site ought to form a metastable, hydrogenic state with a delocalized, VB-like hole weakly bound to a Mu^-_T core. Unlike the shallow Mu donor, spin-orbit interactions and the *p*-orbital character at the VB maximum are likely to hinder measurements of the complex shallow acceptor HF distribution.

Aside from determining H(Mu) dopant properties from where the donor and acceptor levels are located with respect to the host's band gap, extracting the Mu[+/−] level from our results provides a convenient test of the prediction that H[+/−] is pinned at a universal energy with respect to vacuum.[3] This prediction by Van de Walle and Neugebauer has been examined with μSR by Lichti *et al.*[26] for a variety of groups IV, III-V, and II-IV semiconductors. Using band offsets from the work of Van de Walle and Neugebauer, the extrapolated Mu[+/−] levels are fairly uniform with respect to vacuum; the Mu[+/−] level determined from experiment, however, is offset roughly 0.5 eV above their predicted H[+/−] level. This offset is not fully accounted for by isotopic differences between H and Mu. The present results give a test of the Mu[+/−] pinning level in a fully miscible binary alloy system.

TABLE I. Muonium defect energies determined by HTF-μSR and RF-μSR.

Sample	$E_C - E_D$ (meV)	$E_A - E_V$ (meV)	U (meV)
Si[a]	210 ± 10	520 ± 40	-390 ± 41
$Si_{0.80}Ge_{0.20}$	206 ± 4		
$Si_{0.55}Ge_{0.45}$	219 ± 76		
$Si_{0.23}Ge_{0.77}$	332 ± 27	128 ± 8	-385 ± 28
$Si_{0.19}Ge_{0.81}$	302 ± 37	116 ± 8	-432 ± 38
$Si_{0.16}Ge_{0.84}$	340 ± 74	73 ± 10	-437 ± 75
$Si_{0.10}Ge_{0.90}$		22 ± 2	
$Si_{0.09}Ge_{0.91}$	264 ± 36	4.5 ± 1	-461 ± 36
$Si_{0.06}Ge_{0.94}$	198 ± 45		
$Si_{0.02}Ge_{0.98}$	153 ± 5		
Ge[b]	145 ± 7	-80 ± 10	-593 ± 12

[a]References 7 and 8.
[b]References 12 and 13.

Figure 6 displays a band alignment diagram of Mu in $Si_{1-x}Ge_x$ with measured donor and acceptor levels. Where both ionization energies are known for a given alloy, we

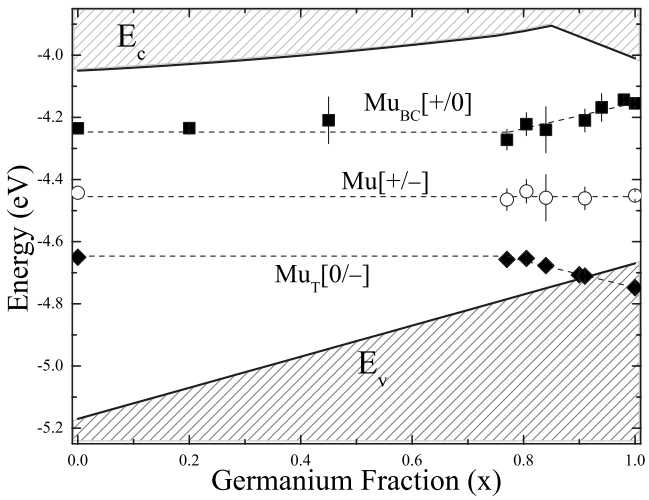

FIG. 6. Band-alignment diagram of donor and acceptor levels in $Si_{1-x}Ge_x$. The energy scale is set by accepted electron affinities for Si and Ge with the conduction band varying smoothly between the two.

have displayed resulting Mu[+/−] levels as open circles. With the conduction-band minimum for Si and Ge placed at the respective electron affinity[27] and a linear variation in VB maximum in the alloys, these results are consistent with a universally pinned Mu transition level at -4.45 ± 0.04 eV below vacuum. Unlike the predictions of Van de Walle and Neugebauer[3] from first-principles calculations that place the H[+/−] in the valence band for pure Ge, our muonium results indicate that Mu[+/−] lies deep in the band gap across the full alloy composition range even though we find that Mu[0/−] does become valence-band resonant for Ge-rich alloys. Our results for Ge-rich alloys are consistent with the charge neutrality level (CNL) in Ge calculated by Tersoff[28] assuming equivalence between this CNL and H[+/−]. The CNL determined by Tersoff is 180 meV above the valence band maximum in Ge as opposed to the results of Van de Walle and Neugebauer that place H[+/−] near 250 meV below the band edge. Accounting for a roughly 50 meV difference in zero-point energy of muonium compared to hydrogen in Ge, our results for Mu[+/−] agree with the work of Tersoff. Our results are inconsistent with the claims[3] that H[+/−] is valence-band resonant in Ge, which would imply that only H^- is thermodynamically stable for any Fermi energy. The present work, however, is indeed consistent with the DLTS results of Dobaczewski *et al.*[11] for the H donor level in Ge and the lack of a DLTS signal associated with the acceptor level. Figure 6 illustrates our results concerning the compensating behavior of Mu, and likely H, across the full alloy range.

V. CONCLUSION

The unique capabilities of μSR techniques have been implemented to provide pseudoisotopic studies of the transition from deep, compensating behavior of H in Si to its predicted role as a source of conductivity in Ge. In contrast to the predictions that H will act only as an acceptor dopant in Ge, we have found that the Mu psuedoisotope of H is a compensating defect in $Si_{1-x}Ge_x$ across the full range of x. Accounting for the small isotopic differences between Mu[+/−] and H[+/−], H ought to likewise behave as a deep, compensating defect for all alloy concentrations. This result rules out shallow acceptor behavior of H as the explanation for problems with hydrogen passivation of acceptors in Ge. These results are consistent with the prior conclusion that passivation by isolated H in Ge may be limited by the formation of an H_2 diffusion barrier near the surface.[2] Ultimately, μSR experimentation can only probe monatomic H and the question still remains as to whether the cause of ineffective passivation in Ge and Ge-rich $Si_{1-x}Ge_x$ is due to H_2 and/or the many possible recombination centers. Where possible, we have determined Mu donor and acceptor ionization energies in $Si_{1-x}Ge_x$ from temperature-dependent Mu^0 fractions. We have further illustrated the consistency of Mu[+/−] for samples where both ionization energies have been determined. More accurate results from first-principles calculations and future μSR experiments are needed for a more comprehensive study of monatomic H-defect characteristics in these technologically important materials.

ACKNOWLEDGMENTS

We would like to thank both the ISIS and TRIUMF facilities for beam time and assistance, as well as, the National Science Foundation [Grant No. DMR-0604501 (R.L.L.)], the Welch Foundation [Grant No. D-1321 (R.L.L.)], the Natural Sciences and Engineering Research Council of Canada (K.H.C.), and the Science and Technology Facilities Council of U.K. (P.J.C.K.).

*bcarroll@astate.edu
†Also at Department of Chemistry and Physics, Arkansas State University, Jonesboro, AR 72401, USA.

[1] J. R. Weber, A. Janotti, P. Rinke, and C. G. Van de Walle, Appl. Phys. Lett. **91**, 142101 (2007).
[2] S. K. Estreicher and D. M. Maric, Phys. Rev. Lett. **70**, 3963 (1993).
[3] C. G. Van de Walle and J. Neugebauer, Nature (London) **423**, 626 (2003).
[4] E. E. Haller, B. Joos, and L. M. Falicov, Phys. Rev. B **21**, 4729 (1980).
[5] R. N. Pereira, B. Bech Nielsen, J. Coutinho, V. J. B. Torres, and P. R. Briddon, Appl. Phys. Lett. **88**, 142112 (2006).
[6] K. Chow, B. Hitti, and R. Kiefl, in *Identification of Defects in Semiconductors*, Semiconductors and Semimetals Vol. 51, edited by M. Stavola (Elsevier, New York, 1998), pp. 137–207, Part 1.
[7] S. R. Kreitzman, B. Hitti, R. L. Lichti, T. L. Estle, and K. H. Chow, Phys. Rev. B **51**, 13117 (1995).
[8] B. Hitti, S. R. Kreitzman, T. L. Estle, E. S. Bates, M. R. Dawdy, T. L. Head, and R. L. Lichti, Phys. Rev. B **59**, 4918 (1999).
[9] B. Holm, K. Bonde Nielsen, and B. Bech Nielsen, Phys. Rev. Lett. **66**, 2360 (1991).
[10] K. Bonde Nielsen, L. Dobaczewski, S. Søgård, and B. Bec Nielsen, Phys. Rev. B **65**, 075205 (2002).
[11] L. Dobaczewski, K. Bonde Nielsen, N. Zangenberg, B. Bech Nielsen, A. R. Peaker, and V. P. Markevich, Phys. Rev. B **69**, 245207 (2004).
[12] R. L. Lichti, S. F. J. Cox, K. H. Chow, E. A. Davis, T. L. Estle, B. Hitti, E. Mytilineou, and C. Schwab, Phys. Rev. B **60**, 1734 (1999).
[13] R. L. Lichti, K. H. Chow, J. M. Gil, D. L. Stripe, R. C. Vilao, and S. F. J. Cox, Physica B **376-377**, 587 (2006).
[14] H. J. Stein, Phys. Rev. Lett. **43**, 1030 (1979).
[15] M. Budde, G. Lupke, C. P. Cheney, N. H. Tolk, and L. C. Feldman, Phys. Rev. Lett. **85**, 1452 (2000).
[16] P. J. C. King, R. L. Lichti, B. R. Carroll, Y. G. Celebi, K. H. Chow, and I. Yonenaga, Physica B **401-402**, 617 (2007).
[17] P. J. C. King, R. L. Lichti, and I. Yonenaga, Physica B **340-342**, 835 (2003).
[18] P. J. C. King, R. L. Lichti, S. P. Cottrell, I. Yonenaga, and B. Hitti, J. Phys.: Condens. Matter **17**, 4567 (2005).
[19] W. Kaiser, P. Keck, and C. Lange, Phys. Rev. **101**, 1264 (1956).

[20] E. Artacho, F. Ynduráin, B. Pajot, R. Ramírez, C. P. Herrero, L. I. Khirunenko, K. M. Itoh, and E. E. Haller, Phys. Rev. B **56**, 3820 (1997).
[21] I. Yonenaga, M. Nonaka, and N. Fukata, Physica B **308-310**, 539 (2001).
[22] S. F. J. Cox, J. Phys.: Condens. Matter **15**, R1727 (2003).
[23] I. Fan *et al.*, Phys. Rev. B **78**, 153203 (2008).
[24] R. C. Vilão, J. M. Gil, A. Weidinger, H. V. Alberto, J. Piroto Duarte, N. Ayres de Campos, R. L. Lichti, K. H. Chow, S. P. Cottrell, and S. F. J. Cox, Phys. Rev. B **77**, 235212 (2008).
[25] B. R. Carroll, R. L. Lichti, P. J. C. King, Y. G. Celebi, I. Yonenaga, and K. H. Chow, Physica B **404**, 812 (2009).
[26] R. L. Lichti, K. H. Chow, and S. F. J. Cox, Phys. Rev. Lett. **101**, 136403 (2008).
[27] *Handbook on Semiconductor Parameters*, edited by M. Levinshtein, S. Rumyantsev, and M. Shur (World Scientific, Singapore, 1996).
[28] J. Tersoff, Phys. Rev. B **30**, 4874 (1984).